Comparison of forecasts of mean monthly water level in the Paraguay River, Brazil, from two fractionally differenced models

Taiane S. Prass,[1] Juan Martin Bravo,[2] Robin T. Clarke,[2] Walter Collischonn,[2] and Sílvia R. C. Lopes[1]

Received 5 September 2011; revised 25 January 2012; accepted 15 March 2012; published 5 May 2012.

[1] The paper compares forecasts of mean monthly water levels up to six months ahead at Ladário, on the Upper Paraguay River, Brazil, estimated from two long-range dependence models. In one of them, the marked seasonal cycle was removed and a fractionally differenced model was fitted to the transformed series. In the other, a seasonal fractionally differenced model was fitted to water levels without transformation. Forecasts from both models for periods up to six months ahead were compared with forecasts given by simpler "short-range dependence" Box-Jenkins models, one fitted to the transformed series, the other a seasonal autoregressive moving average (ARMA) model. Estimates of parameters in the four models (two "long-range dependence", two "short-range dependence") were updated at six-monthly intervals over a 20 year period, and forecasts were compared using root mean square errors (rmse) between water-level forecasts and observed levels. As judged by rmse, performances of the two long-range dependence models, and of the ARMA (1,1) short-range dependence model, were very similar; all three out-performed the seasonal short-range dependence ARMA model. There was evidence that all models performed better during recession periods, than on the hydrograph rising limb.

Citation: Prass, T. S., J. M. Bravo, R. T. Clarke, W. Collischonn, and S. R. C. Lopes (2012), Comparison of forecasts of mean monthly water level in the Paraguay River, Brazil, from two fractionally differenced models, *Water Resour. Res.*, *48*, W05502, doi:10.1029/2011WR011358.

1. Introduction

[2] This paper concerns the long-term behavior of the Paraguay River, a major tributary (area more than 1.0×10^6 km^2, length more than 2600 km) of the immense la Plata drainage system (total area over 4.1×10^6 km^2) of South America (see Figure 1). The la Plata has two other major tributaries: the Paraná River, even larger than the Paraguay, with area over 2.5×10^6 km^2, and the rather smaller Uruguay River; both the Paraná and the Uruguay are major sources of hydropower, which at present supplies more than 70% of Brazil's total energy requirement. At least since the time of *Darwin* [1839], the Paraná River in particular has long been known to exhibit extended periods of flooding, alternating with extended periods of drought, about which Darwin wrote "These droughts to a certain degree seem to be almost periodical; I was told the dates of several others, and the intervals were about fifteen years." However, inspection of Darwin's field notebooks gives no information about how he reached this conclusion. If an extended period of drought were to occur at the present time, the loss of hydropower would severely affect the steadily growing Brazilian economy, while for planning the efficient use of water used to generate energy, forecasts of flow with a lengthy lead time are very desirable. There is a particular concern because during a period of about 12 years starting in the 1960s, flow declined very markedly in the Paraguay River, leading to significant changes in land use. Land became occupied which was apparently no longer subject to the seasonal flooding, hitherto a marked characteristic of the hydrologic regime. As shown later in this paper, at the end of this period the original pattern of seasonal flooding returned, causing economic loss.

[3] As mentioned, the Paraná River—the largest of the three major la Plata tributaries—has been extensively developed for hydropower generation, so that river flows along its length has been greatly modified, and natural flows are difficult to calculate since flow is passed from one impoundment to the next. But it is in the Paraná River basin that extended periods of low flow would have their most severe economic consequences. By contrast, the Paraguay River (see Figure 1), flowing mainly from north to south through the more remote interior of the South American landmass, is free from impoundments, and there is a long record of water level (Figure 2) dating from the beginning of 1900 at the Ladário site, on that river. Figure 1 also shows the extent of the Upper and Lower Paraguay basins into which the Paraguay River basin as a whole is subdivided; the division is defined by the section where the Apa River joins the Paraguay, at the Brazil-Paraguay border. The Ladário gauging station is sited in the Upper Paraguay. It is the long record at Ladário that is used in this paper to explore the utility of long-range dependence stochastic

[1]Instituto de Matemática, Universidade Federal do Rio Grande do Sul, Porto Alegre-RS, Brazil.
[2]Instituto de Pesquisas Hidráulicas, Universidade Federal do Rio Grande do Sul, Porto Alegre-RS, Brazil.

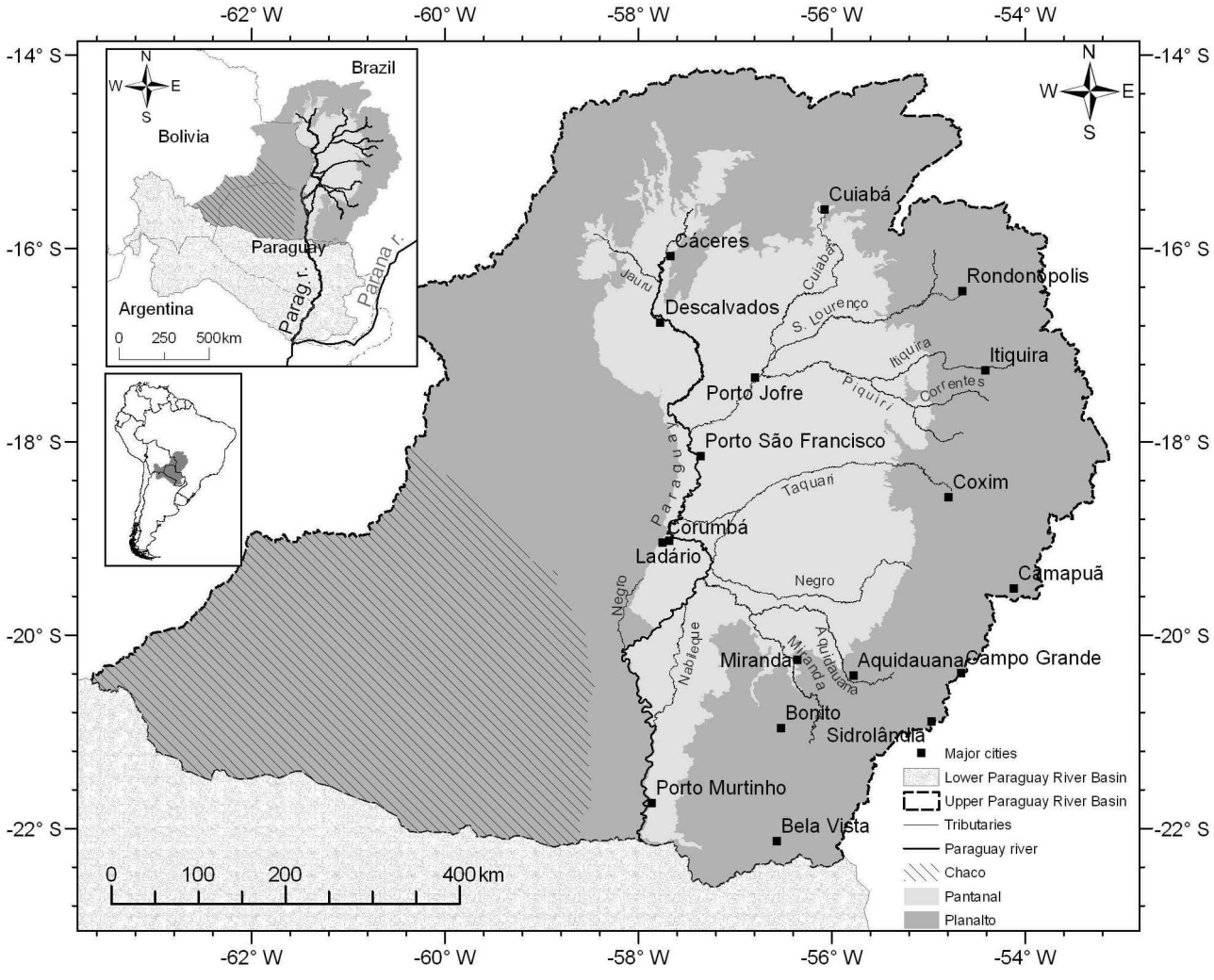

Figure 1. Geographical location of the Upper and Lower Paraguay basins, and of the Ladário gauging station.

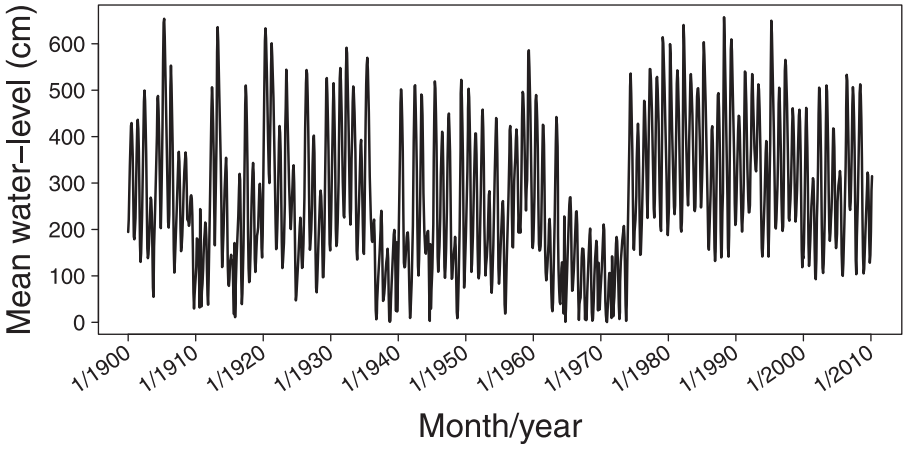

Figure 2. Mean monthly water levels of the Paraguay River at Ladário in the period from January 1900 to March 2010.

models for forecasting purposes in the Paraguay River. Because of the complicated nature of the channel cross section at Ladário, no rating curve exists for the site, so that the analysis which follows is based on the water-level record; this has been read daily since the start of the last century and is remarkably complete for a site of such remoteness. As a first step toward exploring the utility of stochastic long-range dependence models for forecasting flow characteristics in the Paraguay River and possibly elsewhere in the la Plata basin, the long sequence of daily Ladário water levels was used to derive a sequence of mean monthly water levels, and it is this sequence that is used in the rest of the paper. Henceforth we shall refer to this series as the Ladário time series.

[4] *Beran* [1994] sets out the advantages of defining a "physical" mechanism for data sequences that exhibit persistence, and one such model, due to *Granger* [1980], gives a plausible physical justification for long-range dependence in terms of the aggregation of many short-range dependence processes. Granger's model concerns properties of the sum $X_t = \sum_{j=0}^{\infty} Y_t(j)$, in which the time series $\{X_t\}_{t\in\mathbb{N}}$ is the sum of an infinite number of individual time series that are both stationary and short-range dependent. Granger showed that if the short-range dependence processes are independent lag-one autoregressive of the form $Y_t(j) = \alpha_j Y_{t-1}(j) + \varepsilon_t(j)$, with $-1 < \alpha_j < 1$, $\{\varepsilon_t(j)\}_{t\in\mathbb{N}}$ a sequence of independent random variables with variances $\mathrm{Var}(\varepsilon_t(j)) = \sigma_t^2$, for all $j, t \in \mathbb{N}$, then the aggregated process $\{X_t\}_{t\in\mathbb{N}}$ has long-range dependence. This result is attractive because the drainage basin of the Upper Paraguay River basin consists of a large number of distinct subbasins, each with a large number of hydrologic elements (vegetation canopies; slope elements; ...) for which the assumption of linear-reservoir-like behavior [change of storage proportional to input minus output, $dS/dt = p(t) - q(t)$, with output proportional to storage, $S = k \cdot q(t)$] may not be unreasonable. From such physical considerations, therefore, it can be argued that the sequence of Paraguay River water levels at Ladário should be a realization of a long-range dependence process. In the broader context of all rivers, *Mudelssee* [2007] showed by simulation that a river network aggregates short-range dependence precipitation and converts it into long-range dependent runoff, while *Hirpa et al.* [2010] state that "watershed area is an important factor in the long-memory studies of streamflow such as streamflow production"; and the Upper Paraguay is large in terms of area.

[5] Two approaches to modeling long-term persistence in the Ladário time series are used in this paper. One is to use a seasonal fractionally differenced model (SARFIMA: see below) fitted directly to the time series of mean monthly water levels; its advantage is that it is relatively parsimonious in terms of model parameters, but its disadvantage is that it requires monthly variances to be homogeneous, and in general this requirement will not always be hydrologically appropriate. The second alternative, perhaps the one most commonly used in the literature [*Grimaldi*, 2004; *Montanari et al.*, 1997, 2000] is to "deseasonalize" the time series by subtracting the appropriate monthly means and dividing by monthly standard deviations; the deseasonalized series is then regarded as a realization of a simpler fractionally differenced autoregressive fractionally integrated moving average (ARFIMA) model. Seasonality must be reintroduced when such a model is used for forecasting by multiplying by monthly standard deviations and adding monthly means. The ARFIMA model is relatively prodigal in terms of parameters, since 24 (12 monthly means; 12 standard deviations) are required for deseasonalization, in addition to those of the ARFIMA model itself. If confidence intervals were to be required for forecasts, these intervals would need to take account not only of uncertainties in the ARFIMA model parameters, but also the uncertainties in estimates of the seasonality parameters. In this paper, both seasonal autoregressive fractionally integrated moving average (SARFIMA) and ARFIMA models are explored and compared, and they are also compared with models (SARMA and ARMA) for which there is no fractional differencing.

[6] The paper is organized as follows. Section 2 describes the hydrologic regime of the Upper Paraguay River and the Ladário time series. Statistical properties of this time series are discussed in the preliminary analysis presented in section 3. Section 4 presents the main results on model identification, parameter estimation, and forecasting for SARFIMA models. Section 5 presents the results on model identification and parameter estimation for the Ladário time series. This section also compares results from the best-fitting seasonal model SARFIMA for long-term persistence with those from the best-fitting ARFIMA model, and results from both models are compared with those from SARMA and ARMA models which do not model long-term persistence; these latter comparisons show whether inclusion of fractional difference parameters in the models is justified. Section 6 compares the forecasting performance of short-range and long-range dependence models for the first semester of each year (January–July), the period when the annual hydrograph at Ladário has its rising limb, and for the second semester (July–December), which corresponds roughly to the recession period. Section 7 concludes the paper.

2. Hydrologic Regime of the Upper Paraguay River and the Ladário Time Series

[7] The Upper Paraguay has three distinct regions defined by topography and hydrology: the Planalto (260,000 km^2), the Pantanal (140,000 km^2), and the Chaco (200,000 km^2), as shown by Figure 1. The Planalto lies above the 200 m contour and lies mainly in the eastern and northern parts of the basin. Its climate is relatively wet and it generates about 80% of runoff leaving the Upper Paraguay. The Chaco region, to the west, has low annual rainfall (typically less than 1000 mm per year), and an endorheic and ill-defined river drainage network. Its contribution to total Paraguay discharge is small [*Brasil*, 1997].

[8] Rivers flowing from the Planalto enter the Pantanal where gradients are very low, and large areas are seasonally flooded. Water spreading over the floodplain remains enclosed in shallow lakes [*Bordas*, 1996; *Assine and Soares*, 2004; *Assine*, 2005]. The flood pulse is seasonally marked, with an average annual flooded area of 50,000 km^2 [*Hamilton et al.*, 1996; *Bravo et al.*, 2005], which effectively determines the entire ecosystem [*Junk et al.*, 2006; *Hamilton*,

2002]. Since annual rainfall is less than potential evaporation and drainage is very slow because of shallow gradients [*Tucci et al.*, 1999; *Bordas*, 1996], the Pantanal functions as a large natural hydrologic control on the Paraguay River and its tributaries [*Tucci et al.*, 2005; *Bravo et al.*, 2005; *Paz et al.*, 2011; *Bravo et al.*, 2012]. Although seasonal distribution of rainfall is very similar over the whole Paraguay River basin, with higher rainfall during summer and very low rainfall during winter, peak river flows occur at different times at different points along the Paraguay River. Because of the low slopes and reservoir-like behavior of the Pantanal, flood peaks take several months to progress downstream.

[9] The data set of Ladário gauging station is available on request from the Brazilian National Water Agency ANA. The original data set contains daily measurements of the water level in the Paraguay River at Ladário for the period from January 1900 to March 2010. Since changes in daily water levels are very gradual, monthly mean levels are used throughout this paper. Figure 2 shows the time series of mean monthly water levels $\{X_t\}_{t=1}^{n}$, with $n = 1323$ observations, where $t = 1$ and $t = n$ correspond to January 1900 and March 2010, respectively. The reason for the decline in water level over the extended period from 1960 to about 1975 has never been fully explained, but is replicated in other time series of river flows from other parts of the la Plata drainage system. Figure 3, giving a box plot of mean monthly water level over the period of record, illustrates the general smoothness of the annual hydrograph, with a rising limb extending roughly from January to June, and a recession from July to December. We show that the forecasting models discussed later in the paper tend to perform differently in these two periods.

[10] In what follows, the data set $\{X_t\}_{t=1}^{1323}$ is divided in two subsamples. The subsample $\{X_t\}_{t=1}^{1092}$, corresponding to the period from January 1900 to December 1990, is used for preliminary analysis and for model identification, estimation, and verification, while the subsample $\{X_t\}_{t=1093}^{1323}$ is used to investigate model forecasting performance.

3. Preliminary Analysis of the Ladário Time Series

[11] Here we perform a preliminary analysis of the Ladário time series. The aim of this analysis is to investigate whether the stationarity property holds; to check if the time series has Gaussian distribution (this is not required by most time series models but is required when testing hypotheses); to analyze the existence of a deterministic and/or stochastic seasonal components; and to analyze the decay in the sample autocorrelation function. This information is needed to identify a class of models for the data.

[12] Stationarity is required since long-range dependence models (more generally, linear models) are based on the assumption that the observed time series is a realization of a weak-stationarity process with uncorrelated innovations. Although some models are based on the hypothesis of Gaussianity, most definitions only assume that the innovation process is a white noise, that is, a sequence of noncorrelated random variables with constant mean and variance but not necessarily independent or Gaussian [*Hosking*, 1981; *Brockwell and Davis*, 1991; *Bisognin and Lopes*, 2007].

[13] Since nonstationarity can be caused by a deterministic seasonal component or by a monotonic trend, these hypotheses are investigated. Hydrologic time series commonly present an annual cycle, so it is expected the seasonal period to be equal to 12. Usually this can be confirmed by simple inspection of the time series graph or by observing the length of the cycle in the sample autocorrelation function. Once we have identified the period of seasonality, the seasonal Mann–Kendall test can be applied to investigate the existence of a monotonic trend [*Hipel and McLeod*, 1994]. Furthermore, as a first attempt to

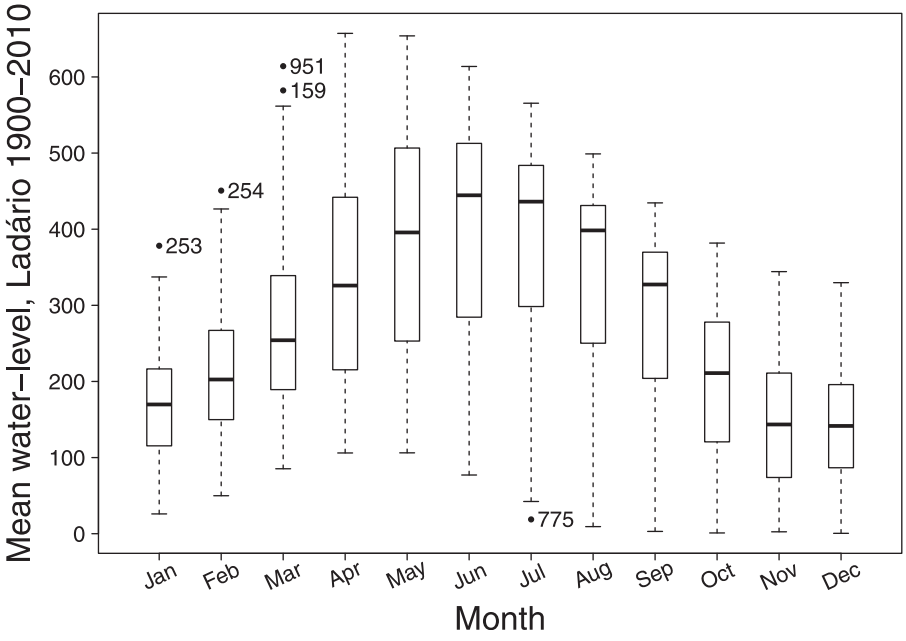

Figure 3. Box plot of mean monthly water level over the period 1900–2010. Numbers against outliers indicate the months in which they occurred, reckoned from January 1900 as month 1.

remove the influence of the annual cycle, a common approach is to transform the data by subtracting monthly means and scaling by monthly standard deviations [*Grimaldi*, 2004; *Montanari et al.*, 1997, 2000]. If the periodicity is caused by a deterministic component, the transformed data should not show seasonality in mean and variance [*Grimaldi*, 2004].

[14] Figure 4(a) shows the sample autocorrelation function (ACF) $\hat{\rho}(h)$ of the Ladário time series for $h = 0, \ldots, 200$. The cyclical behavior in the ACF is evident and indicates a periodic behavior with seasonal period equal to 12. By performing the seasonal Mann–Kendall test, assuming that the seasons are correlated, we obtain the score statistic $S = 1321$, with variance $\mathrm{Var}(S) = 10,201,759$. Therefore, the p value of the test statistic $S/\sqrt{\mathrm{Var}(S)} = 0.4133$ is 0.68 and the null hypothesis of no trend is not rejected. To verify if the periodicity in the data is due to a deterministic component, we consider the transformed time series $\{Y_t\}_{t=1}^{1092}$ as described before, that is

$$Y_{\tau s+i} = \frac{X_{\tau s+i} - m_i}{\sigma_i} \quad \text{for} \quad i = 1, \ldots, 12 \quad \text{and} \quad \tau = 0, \ldots, 90,$$

where $s = 12$ is the period of seasonality, m_i and σ_i are, respectively the overall sample mean and standard deviation for month i, defined as

$$m_i = \frac{1}{N}\sum_{\tau=0}^{N-1} X_{\tau s+i} \quad \text{and} \quad \sigma_i = \frac{1}{N-1}\sum_{\tau=0}^{N-1}(X_{\tau s+i} - m_i)^2,$$

where $N = 91$ is the total number of years in the period from January 1900 to December 1990. These values are presented in Figure 5.

[15] Figures 6(a) and 6(b) show the kernel density function and the "best fitted" Gaussian density function, respectively, for the original Ladário time series and for the deseasonalized time series. Clearly these time series do not have Gaussian distribution. A Box-Cox transformation could be applied so as to obtain a Gaussian time series. However, as reported by *Grimaldi* [2004], the final model obtained after applying such a transformation may not be useful since the inverse Box-Cox transformation may yield very large distortions. The use of the Box-Cox transformation is also discussed by *Montanari et al.* [1997, 2000]. In both papers the authors conclude that the time series considered are well modeled even without transforming the

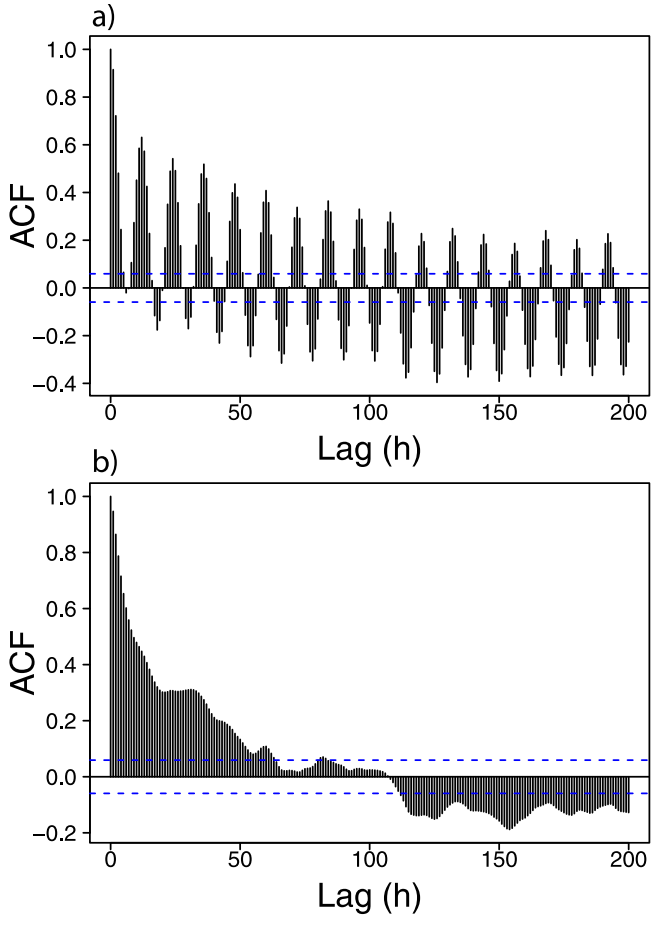

Figure 4. Sample autocorrelation function for lags $h = 0, \ldots, 200$: (a) of the original time series $\{X_t\}_{t=1}^{1092}$ corresponding to the mean monthly water level in the Paraguay River at Ladário in the period from January 1900 to December 1990; (b) of the deseasonalized time series. Dashed lines correspond to the 95% confidence bands.

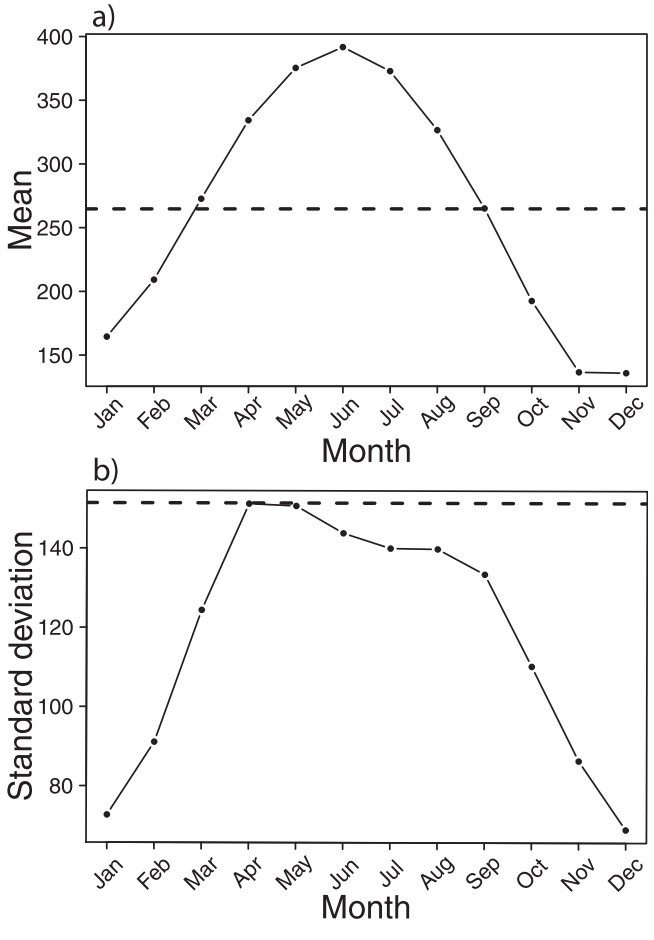

Figure 5. Mean (m_i) and standard deviation (σ_i) by month for the water-level time series for the period from January 1900 to December 1990. Dashed lines correspond to the overall mean/standard deviation.

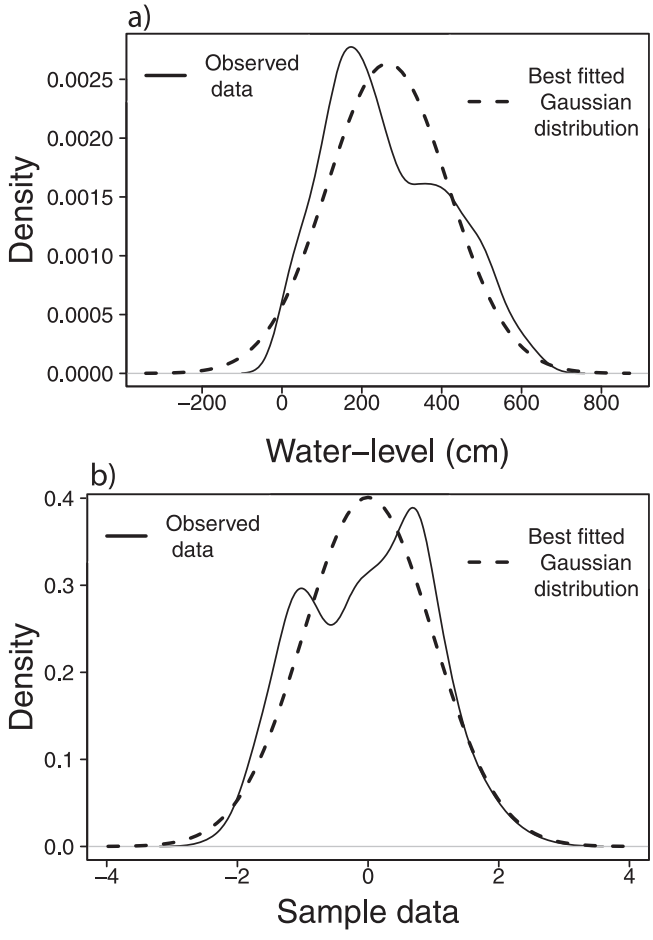

Figure 6. Kernel density funtion and "best fitted" Gaussian density function: (a) for the original Ladário time series; (b) for the deseasonalized time series.

data. Since the fitted model will be used for forecasting, the Box-Cox transformation was not used here.

[16] The next step is to decide whether a class of short-range or long-range dependence model should be considered by looking at the decay in the sample autocorrelation function. While for short-range dependence models this function decays rapidly or is zero for $h > h_0$ (as in MA models), for some $h_0 > 0$, for long-range dependence models it decays very slowly. From Figures 4(a) and 4(b) we conclude that for both the original and deseasonalized Ladário time series, the decay of the sample autocorrelation functions is very slow, which indicates long-range dependence.

[17] Another procedure to detect long-range dependence is the detrended fluctuation analysis (DFA) proposed by *Peng et al.* [1992]. *Crato et al.* [2010] give a full description and technical details of the DFA method, while *Crato et al.* [2011] report an application to DNA sequences and *Livina et al.* [2003] apply the DFA to measure the correlation properties of river flow fluctuations. To apply the DFA method to the original and deseasonalized Ladário time series we considered two different values of $g(n)$ [for details, see *Crato et al.*, 2010], where $n = 1092$ is the sample size. By considering $g(n) = \lfloor n/10 \rfloor$, which is the usual choice in the literature, the scaling exponent α was estimated as $\hat{\alpha} = 0.81$ (original time series) and 1.13 (deseasonalized time series). By considering $g(n) = n^{0.8}$, α was estimated as $\hat{\alpha} = 0.92$ (original time series) and 1.09 (deseasonalized time series). These results indicate that both time series have long-range dependence.

4. Fractionally Differenced Models

[18] An annual cycle is a common characteristic of most hydrologic time series and the literature shows that long-range dependence in mean can sometimes be expected [*Hosking*, 1984; *Montanari et al.*, 1997, 2000; *Bisognin and Lopes*, 2007]. For a stationary stochastic process $\{X_t\}_{t\in\mathbb{Z}}$, the periodicity is usually detected through the oscillating autocorrelations and the long-range dependence is reflected by the hyperbolic decay of the autocorrelation function or by the unboundedness of the spectral density function at the zero frequency. If $\{X_t\}_{t\in\mathbb{Z}}$ also presents seasonal long-range dependence, then the spectral density function is unbounded at the frequencies $2k\pi/s$, $k = 0, 1, 2, \ldots$, where s is the seasonality period.

[19] A common measure of the long-range dependence intensity is the Hurst's coefficient H, which varies between 0 and 1 [*Hurst*, 1951]. Several heuristic procedures are available to detect long-range dependence [*Beran*, 1994]. However, since they only provide estimates for the parameter H, they cannot fully describe the statistical properties of the time series, nor can they be used for forecasting. Parametric models are therefore often considered as an alternative. For example, *Granger and Joyeux* [1980] and *Hosking* [1981] introduced the autoregressive fractionally integrated moving average model, denoted by ARFIMA(p, d, q) or FARIMA(p, d, q) models. These models display long-range dependence when the differencing parameter d is in the interval $(0, 0.5)$, enabling it to reproduce the Hurst phenomenon. Moreover, the parameters d and H are related through the equality $d = H - 1/2$. To account for cyclical behavior, *Porter-Hudak* [1990] introduces the seasonal autoregressive fractionally integrated moving average (SARFIMA) process and *Hassler* [1994] presents a complete generalization of fractional differencing processes with the presence of periodicity considering rigid and flexible models.

[20] The SARFIMA model (also known in the literature as ARFISMA or FARISMA), is a special case of the generalized FARIMA model considered by *Giraitis and Leipus* [1995]. Using the same notation as *Montanari et al.* [2000], *Bisognin and Lopes* [2007, 2009] and *Bisognin* [2007], a SARFIMA$(p, d, q) \times (P, D, Q)_s$ process is defined as the solution of

$$\phi(\mathcal{B})\Phi(\mathcal{B}^s)(1-\mathcal{B})^d(1-\mathcal{B}^s)^D(X_t-\mu) = \theta(\mathcal{B})\Theta(\mathcal{B}^s)\varepsilon_t. \quad (1)$$

When $P = Q = 0$ and $D = 0$, the model in expression (1) reduces to the ARFIMA(p, d, q) model; when $d = 0 = D$, to the so-called SARMA$(p, q) \times (P, Q)_s$ (seasonal ARMA) model; when $P = Q = 0$ and $d = D = 0$, to the ARMA (p, q) model.

[21] In expression (1), $\mu \in \mathbb{R}$ is the process mean, $\{\varepsilon_t\}_{t\in\mathbb{Z}}$ is a white noise process with mean zero and variance σ^2_ε, $s \in \mathbb{N}^*$ is the period of the seasonality, and d and D are, respectively, the nonseasonal and seasonal differencing order parameters (allowed to be fractional). While the

parameter d is related to long-range dependence, as in the ARFIMA(p,d,q) processes, D is the parameter associated with the seasonal long-range dependence. In particular, if $d=0$ and $p=q=P=Q=0$, then X_t and X_{t+h} have zero correlation whenever h is not a multiple of the seasonal period s. If d and D are both nonzero then the process has both long-range dependence and seasonal long-range dependence. Moreover, $\mathcal{B}$ is the backward shift operator defined by $\mathcal{B}^{sk}(X_t)=X_{t-sk}$ for all $k\in\mathbb{N}$, $(1-\mathcal{B})^d$ and $(1-\mathcal{B}^s)^D$ are, respectively, the nonseasonal and the seasonal difference operators. If $D\in\mathbb{N}$, $(1-\mathcal{B}^s)^D$ is simply the seasonal difference operator iterated D times and, for any noninteger $D>-1$, the operator is defined by

$$(1-\mathcal{B}^s)^D=\sum_{k=0}^{\infty}\frac{\Gamma(k-D)}{\Gamma(-D)\Gamma(k+1)}\mathcal{B}^{sk}:=\sum_{k=0}^{\infty}\delta_{D,k}\mathcal{B}^{sk},$$

with $\delta_{D,0}=1$. The operator $(1-\mathcal{B})^d$ is obtained from the above equality when $D=d$ and $s=1$. Furthermore, the polynomials $\phi(\cdot)$, $\theta(\cdot)$ $\Phi(\cdot)$, and $\Theta(\cdot)$, respectively, of degree p, q, P, and Q, describe the nonseasonal and seasonal short-range dependence, as in SARMA$(p,q)\times(P,Q)_s$ processes. While $\phi(\cdot)$ and $\Phi(\cdot)$ are, respectively, the nonseasonal and seasonal autoregressive polynomials, $\theta(\cdot)$ and $\Theta(\cdot)$ are, respectively, the nonseasonal and seasonal moving average polynomials, defined by

$$\phi(z)=\sum_{k=0}^{p}(-\phi_k)\,z^k,\quad \theta(z)=\sum_{k=0}^{q}\theta_k\,z^k,\quad \Phi(z)=\sum_{k=0}^{P}(-\Phi_k)\,z^k,$$
$$\text{and }\ \Theta(z)=\sum_{k=0}^{Q}\Theta_k\,z^k,$$

with $\phi_0=-1=\Phi_0$ and $\theta_0=1=\Theta_0$.

[22] The properties of long-range dependence (and seasonal long-range dependence) models and its applications are well documented in the literature [*Ray*, 1993; *Hassler*, 1994; *Peiris and Singh*, 1996; *Reisen and Lopes*, 1999; *Montanari et al.*, 1997, 2000; *Elek and Márkus*, 2004; *Arteche and Robinson*, 2000; *Palma*, 2007; *Bisognin and Lopes*, 2007; *Bisognin*, 2007]. In particular, *Bisognin and Lopes* [2009] deal with the complete SARFIMA$(p,d,q)\times(P,D,Q)_s$ processes giving proofs of theoretical properties such as the spectral density function expression and its behavior near the seasonal frequencies, the stationarity, the intermediate dependence characteristics, the autocovariance function, and its asymptotic expression. The authors also investigate the ergodicity and present necessary and sufficient conditions for the causality and the invertibility properties of the complete SARFIMA processes.

[23] In practice, the identification of the autoregressive and moving average orders (seasonal and nonseasonal) for SARFIMA (or ARFIMA) models is not straightforward, usually requiring trial and error procedures [*Montanari et al.*, 1997]. A common approach is to obtain a preliminary value for the parameters d and D then use those values to differentiate the time series (by applying a linear filter) and thus to consider the traditional identification methods for SARMA (or ARMA) models. This procedure is commonly used not only to identify the order of the autoregressive and moving average polynomials (seasonal and nonseasonal) but also to provide initial values in the parameter estimation step.

[24] Model parameters can be estimated by maximum likelihood [*Tyralis and Koutsoyiannis*, 2011]. However, computing the exact likelihood function requires knowing the underlying distribution of the data. Therefore, in practice, an approximation of the Gaussian maximum likelihood function in the spectral domain is used instead [*Beran*, 1994]. This approximation was first proposed by *Whittle* [1953] for short-range dependence models. It is well known that the Whittle's estimator yields maximum likelihood estimates only for Gaussian data. In the non-Gaussian case, the method gives least square estimates. In both cases, Gaussian and non-Gaussian, the estimates are asymptotically consistent [see *Montanari et al.*, 2000 and references therein]. Furthermore, simulation studies presented by *Reisen et al.* [2001] and *Sena Jr. et al.* [2006] confirm that the Whittle's estimator performs well for ARFIMA time series with non-Gaussian innovations and sample size $n=300$. In particular, *Reisen et al.* [2001] considers misspecification against heavy-tailed, skewed, and bimodal distributions.

[25] By considering Whittle's method, given a time series $\{X_t\}_{t=1}^n$, the parameter estimation is carried out by minimizing the function $Q(\cdot)$ defined as

$$Q(\boldsymbol{\xi})=\sum_{j=1}^{m}\frac{I_n(\lambda_j)}{f_*(\lambda_j;\,\boldsymbol{\xi})},\tag{2}$$

where $m=\lfloor(n-1)/2\rfloor$, $\lambda_j=2\pi j/n$ for $j\in\{1,\ldots,m\}$ are the Fourier frequencies, $I_n(\cdot)$ is the periodogram function, and $f_*(\cdot,\boldsymbol{\xi})$ is defined by $f(\cdot;\boldsymbol{\eta})=f_*(\cdot;\boldsymbol{\xi})\times\sigma_\varepsilon^2/(2\pi)$, where $\boldsymbol{\eta}=(\sigma_\varepsilon,\xi')'$ is the vector of unknown parameters of the model and $f(\cdot;\boldsymbol{\eta})$ is the spectral density function of a stationary SARFIMA$(p,d,q)\times(P,D,Q)_s$ process, which is given by [*Bisognin and Lopes*, 2009]

$$f(\lambda;\boldsymbol{\eta})=\frac{\sigma_\varepsilon^2}{2\pi}\frac{|\theta(e^{-i\lambda})|^2}{|\phi(e^{-i\lambda})|^2}\frac{|\Theta(e^{-is\lambda})|^2}{|(e^{-is\lambda})|^2}\times|1-e^{-i\lambda}|^{-2d}\times|1-e^{-is\lambda}|^{-2D},$$

for all $\lambda\in[0,\pi]$. The estimator of σ_ε^2 is then given by $\hat{\sigma}_\varepsilon^2=4\pi/n\times Q(\hat{\boldsymbol{\xi}})$, where $\hat{\boldsymbol{\xi}}$ maximizes (2). Notice that this method does not give an estimate $\hat{\mu}$ for the parameter μ. In this work we set $\hat{\mu}=X$, where X is the sample mean of $\{X_t\}_{t=1}^n$.

[26] Once the parameters of the model are estimated, the residuals $\{\hat{\varepsilon}_t\}_{t=1}^n$ are calculated based on the infinite order autoregressive representation of a SARFIMA process, which is given by $\varepsilon_t=\sum_{k=0}^{\infty}\pi_k X_{t-k}$, where the coefficients π_k for all $k\in\mathbb{N}$ are defined by

$$\sum_{k=0}^{\infty}\pi_k z^k=\frac{\phi(z)\Phi(z^s)}{\theta(z)\Theta(z^s)}(1-z)^d(1-z^s)^D.\tag{3}$$

Moreover, by letting $\hat{X}_t := X_t - \hat{\varepsilon}_t$ for all $t \in \{1, \ldots, n\}$ we obtain the fitted values (also termed the in-sample forecast). Hence, classical goodness-of-fit tests can be performed to verify the validity of the model and/or to provide a final decision rule if more than one model is shown to fit the data well.

[27] The forecasting equations for SARFIMA (ARFIMA) models are simple. Without loss of generality, assume $\mu = 0$. Then, with respect to the mean square error, the best linear predictor of X_{n+h}, based on $\mathcal{F}_n := \sigma(\{X_s\}; s \leq n)$, is given by $\hat{X}_{n+h} = \mathbb{E}(X_{n+h}|\mathcal{F}_n)$, which can be written as [*Bisognin*, 2007]

$$\hat{X}_{n+h} = -\sum_{k=1}^{\infty} \pi_k \hat{X}_{n+h-k}, \tag{4}$$

where $\hat{X}_{n+h-k} = X_{n+h-k}$, whenever $h - k \leq 0$, and $\{\pi_k\}_{k\in\mathbb{N}}$ is defined in (3).

[28] The forecasting performance of a model is commonly evaluated by calculating the mean absolute error (*mae*), the root mean square error (*rmse*) or the mean absolute percentage error of forecast (*mape*) values, respectively defined as

$$mae = \frac{1}{n_p}\sum_{h=1}^{n_p} |e_{n+h}|, \quad rmse = \sqrt{\frac{1}{n_p}\sum_{h=1}^{n_p} |e_{n+h}|^2}, \quad \text{and} \quad mape = \frac{1}{n_p}\sum_{h=1}^{n_p} \frac{|e_{n+h}|}{|X_{t+h}|}, \tag{5}$$

where $e_{n+h} = X_{n+h} - \hat{X}_{n+h}$ is the forecasting error, n is the forecasting origin, and n_p is the total number of predicted values. The *mape* is a good measure since it considers not only the magnitude of the error (as do the *mae* and the *rmse*) but also the proportion between the error and the true values so it is easier to decide whether the error is small or not. A drawback is that this measure is highly affected when observations are close to zero.

5. Model Identification and Estimation on the Ladário Time Series

[29] As shown above, preliminary analysis of the Ladário time series suggests the use of long-range dependence models, and we consider here the ARFIMA(p, d, q) model for the deseasonalized time series $\{Y_t\}_{t=1}^{1092}$ and, for comparison, a SARFIMA$(p, d, q) \times (P, D, Q)_s$ model for the original time series $\{X_t\}_{t=1}^{1092}$. To assess whether forecasts of Ladário mean monthly water level were improved by including the persistence parameters d and D, simple ARMA and seasonal ARMA (SARMA) models were also fitted.

[30] All models were identified using the mean monthly water levels for the years 1900–1990 inclusive, 1092 values in all. SARFIMA and SARMA models were fitted to these values, but ARFIMA and ARMA models were fitted to the deseasonalized series, as explained earlier. Monthly observations for the years 1991–2010 (20 years) were used to compare with forecasts obtained from the fitted models. The reverse transformation was considered when calculating the *mae*, *mape*, and *rmse* between observed and predicted values.

[31] Six ARFIMA(p, d, q) models were fitted for all combinations of $p, q \in \{0, 1, 2\}$. The model with $p = q = 0$ was excluded given the high value of the Portmanteau test statistic $Q(100) = 913$ (the critical value for the test is 124.34). The Bayes Information Criterion (BIC) was then used to select the best model. The model ARFIMA$(1, d, 1)$ gave the smallest BIC (-2588.26) and the smallest *mape* (0.21) values when the latter was calculated from the remaining 20 years of monthly data, after fitting the model. The value of d for this model was $d = 0.35 \pm 0.096$, corresponding to a Hurst coefficient of $H = 0.85$. Estimates of the AR and MA parameters were 0.691 ± 0.081 and 0.228 ± 0.042, respectively, both exceeding twice their standard errors.

[32] The SARFIMA models were fitted for all combinations of $p, q, P, Q \in \{0, 1, 2\}$. We also consider the models with $d = 0$ or $D = 0$ (fixed). The Portmanteau test rejected the null hypothesis that the residuals were statistically independent for all SARFIMA models. Similar results were found by *Montanari et al.* [1997] and *Grimaldi* [2004]. Thus the test could not be used as a model selection criteria. The model with very high BIC values (>8100) were discarded together with others for which estimates of the long-range dependence parameters d and D were greater than 0.5, giving models that were not stationary; 26 candidate models remained. Models with more than six parameters were then eliminated (seven candidates remained) and the cumulative periodogram test on the residuals of these seven SARFIMA models was used as a final selection procedure. Finally, four candidate models remained. The goodness-of-fit statistics for these four models are given in Table 1. As shown in Table 1, values of BIC and *mape* (in-sample and out-of-sample) did not vary much among the

Table 1. Bayesian Information Criteria (BIC), Portmanteau Test Statistic $Q(100)$, Shapiro-Wilk Test Statistic, *mae*, *mape*, and *rmse* for Four Competitive SARFIMA Models Fitted to the Ladário Time Series[a]

Model	S1	S2	S3	S4
BIC	8031.657	8015.065	7987.431	7977.565
$Q(100)$	337.190	290.750	192.100	165.400
Shapiro-Wilk	0.903	0.903	0.905	0.905
mae[b]	26.072 (71.670)	25.884 (73.927)	25.755 (67.415)	25.792 (64.442)
mape[b]	0.352 (0.281)	0.403 (0.265)	0.402 (0.249)	0.400 (0.243)
rmse[b]	39.027 (86.670)	38.856 (91.473)	38.245 (81.807)	38.073 (77.256)

[a]All models have less than six parameters and noncorrelated residuals according to the cumulative periodogram test. By definition, S1 = SARFIMA$(1, d, 1) \times (0, D, 0)_{12}$, S2 = SARFIMA$(2, d, 0) \times (0, D, 0)_{12}$, S3 = SARFIMA$(2, d, 0) \times (1, D, 0)_{12}$, and S4 = SARFIMA$(2, d, 0) \times (0, D, 1)_{12}$.
[b]The values in parentheses correspond to the respective statistics calculated based on the 231 predicted and observed values (not used for model identification or fitting).

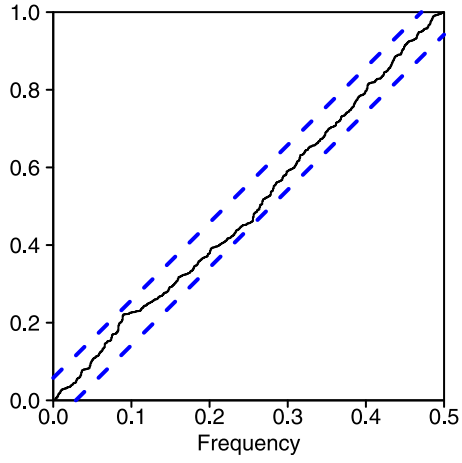

Figure 7. Cumulative periodogram test on the residuals of the SARFIMA$(2,0,0)\times(0,D,1)_{12}$ model applied to the Ladário time series. Dashed lines correspond to the 95% confidence bands.

tested models. By comparing *mae* and *rmse* the model selected was SARFIMA$(2,0,0)\times(0,D,1)_{12}$ for which the value of $\hat{D}$ was 0.439 ± 0.035. The parameters ϕ_1, ϕ_2, and Θ_1 were estimated as 1.300 ± 0.028, $-0.391\pm0.0.028$, and -0.334 ± 0.048, respectively. The cumulative periodogram test on the residuals of this model is presented in Figure 7.

[33] For both ARFIMA and SARFIMA models, a Shapiro-Wilks test was used to test whether model residuals could be considered normally distributed, but the hypothesis of normality was rejected for both models. A summary of the estimation results for the four models ARFIMA$(1,d,1)$, ARMA$(1,1)$, SARFIMA$(2,0,0)\times(0,D,1)_{12}$, and SARMA$(2,0)\times(0,1)_{12}$ is presented in Table 2. Table 3 shows goodness-of-fit statistics for these four models, for the remaining 231 values in the Ladário time series which were not used for model identification and estimation.

Table 3. Performance Measures for Four Models Used to Estimate 231 Observations Not Used for Model Identification or Fitting

Model	Criteria		
	mae (cm)	*mape* (%)	*rmse* (cm)
ARFIMA$(1,d,1)$	59.40	21.13	73.04
ARMA$(1,1)$	70.90	22.60	87.13
SARFIMA$(2,0,0)\times(0,D,1)_{12}$	66.44	24.34	77.26
SARMA$(2,0)\times(0,1)_{12}$	109.40	38.20	135.44

[34] Table 3 suggests that the performance of the SARMA model is appreciably worse than that of any other three, although in all models both *mae* and *rmse* values are large, as would be expected for estimates at such large lead times. Setting aside the poor performance of the SARMA model, Table 3 suggests that there is not much difference among the performance of the remaining three models ARFIMA$(1,d,1)$, ARMA$(1,1)$, and SARFIMA$(2,0,0)\times(0,D,1)_{12}$, although, by all three performance measures, the latter model performed less well than the ARFIMA$(1,d,1)$ fitted to the normalized residuals of the time series. The relatively good performance of the simple ARMA(1, 1) model, even when it has been shown that estimates of the long-range dependence parameters d and D are significantly greater than zero, is not surprising in view of the very marked seasonal fluctuation in mean monthly water level shown by the box plot in Figure 3; when seasonality is reintroduced into estimates $\hat{Y}_{n+h}$, where $n=1092$ and $h\in\{1,\ldots,231\}$ with $n+h=\tau s+i$ for some $\tau\in\{0,\ldots,19\}$ and $i\in\{1,\ldots,12\}$, by the inverse transformation $\hat{X}_{t+h}=m_i+\sigma_i\hat{Y}_{t+h}$, the major part of the signal in mean monthly water level is thereby incorporated. And since the serial correlation among the normalized residuals is high, an ARMA(1, 1) model fitted to them would be expected to show persistence characteristics similar to those of fractionally differenced models [*O'Connell*, 1973]. On the other hand, the relatively poor performance of the SARMA model, shown in Table 3

Table 2. Estimated Parameters (in Parentheses, the SE of the Estimate) and Goodness-of-Fit Test Statistics for the ARFIMA(1, *d*, 1), ARMA(1, 1), SARFIMA(2, 0, 0) × (0, *D*, 1)$_{12}$ and SARMA(2, 0) × (0, 1)$_{12}$ Models[a]

Estimate	Model			
	ARFIMA	ARMA	SARFIMA	SARMA
$\hat{d}$	0.350 (0.096)	–	–	–
$\hat{D}$	–	–	0.439 (0.035)	–
$\hat{\phi}_1$	0.692 (0.080)	0.915 (0.013)	1.300 (0.028)	1.516 (0.023)
$\hat{\phi}_2$	–	–	−0.391 (0.028)	−0.658 (0.023)
$\hat{\theta}_1$	0.228 (0.042)	0.350 (0.030)	–	–
$\hat{\Theta}_1$	–	–	−0.334 (0.048)	0.185 (0.030)
$\hat{\sigma}_\varepsilon$	0.091	0.092	1411.275	1762.808
$\hat{\mu}$	0.000	0.000	264.729	264.729
mae (cm)	22.61	22.76	27.79	27.98
mape	0.34	0.34	0.40	0.47
rmse (cm)	33.24	33.26	38.07	42.10
$Q(100)$	87.93	95.84	165.40	848.43
Shapiro-Wilk	0.90[b]	0.90[b]	0.90[b]	0.90[b]

[a]The *mae*, *mape*, and *mse* values correspond to the in-sample forecast (set $h=0$ in the definition). For the ARFIMA and ARMA the *mae*, *mape*, and *mse* values were calculated after performing the inverse transformation $\hat{X}_{\tau s+i}=m_i+\sigma_i\hat{Y}_{\tau s+i}$ for all $\tau=1,\ldots,90$ and $i=1,\ldots,12$, with $s=12$. The critical value for the Portmanteau test is 124.34 (confidence level $\alpha=0.95$).

[b]Corresponding p value is equal to 0.

and confirmed below, may be associated with inhomogeneity in the 12 monthly variances; the box plot of Figure 3 shows that dispersion may be greater in months when water levels are also high.

[35] Table 3 gives results obtained when models fitted to the first 1092 values (the period 1900–1990) in the Ladário time series, and are then used to estimate remaining values in the sequence (the period 1991–2010). Of greater interest from a practical point of view is how easily model parameters and forecasts can be updated on a regular basis, and this topic is covered in section 6.

6. Results of Updating Estimates of Model Parameters and Forecasts

[36] From a user's perspective, important questions are "how easy is it to update estimates of parameters in a fractionally differenced model, and to update the forecasts obtained from it?" and "how do forecasts of hydrologic variables, obtained by recursively updating forecasts from fractionally differenced models, compare with forecasts given by ordinary ARMA models, seasonal or otherwise, that are in widespread use?". These questions must be addressed if such models are to find use as a practical forecasting procedure for hydrologic use, but to the authors' knowledge, they have not been addressed in the literature.

[37] As a partial response to the first question, the authors' experience is that minimization of the expression $Q(\cdot)$ in equation (2) is very rapid, taking no more than a few seconds on an ordinary laptop computer (although there maybe problems of convergence if p, q, P, Q are not small integers). It is certainly very much faster, in our experience, than use of the approximate maximum likelihood method in the time domain, given by *Beran* [1994, section 5.6], for which problems of convergence were encountered even when $P = Q = 0$, $p = q = 1$. Thus provided the model does not have many parameters, calculating updates of parameters should not be difficult. Similarly, the updating of forecasts using equation (4) is straightforward.

[38] To address the second question, forecasts from four models with the same autoregressive and moving average orders (seasonal and nonseasonal) as those in section 5 were compared, by calculating root mean square errors (rmse) between the forecasts obtained from them, and the observed mean monthly water levels, in successive six-monthly periods as described below. Models 1 and 2 were fitted to the deseasonalized time series and models 3 and 4 were fitted to the original time series, where

Model 1: ARFIMA$(1, d, 1)$;
Model 2: ARMA$(1, 1)$;
Model 3: SARFIMA$(2, 0, 0) \times (0, D, 1)_{12}$;
Model 4: SARMA$(2, 0) \times (0, 1)_{12}$.

[39] Thus model 1 has nonzero fractional-differencing parameter d, model 3 has $d = 0$ and nonzero seasonal fractional-differencing parameter D, while in models models 2 and 4 both d and D parameters are set equal to zero, so that models 2 and 4 are simply ordinary ARMA and SARMA models without long-range dependence. Model 4 does not satisfy the hypothesis of noncorrelated residuals and is used only for comparison.

[40] To compare forecasts given by the four models, with updating, the following procedure was used:

[41] 1. Each model was fitted using the time series up to December 1990 ($n = 1092$), and forecasts $\hat{X}_{n+1}, \ldots, \hat{X}_{n+6}$, with forecasting origin $n = 1092$, of mean monthly water level, were calculated for the period January–June 1991 (i.e., the following six-months period).

[42] 2. The rmse between model forecasts and observed mean water levels were calculated for each model over this period, according to expression (5).

[43] 3. Using the time series up to the end of June 1991 ($n = 1098$), the parameters of each model were recalculated, thus recalibrating the model, and forecasts $\hat{X}_{n+1}, \ldots, \hat{X}_{n+6}$, with forecasting origin $n = 1098$, were made for the period July–December 2001.

[44] 4. As in step 2 above.

[45] 5. The calculation was repeated for the six-monthly intervals extending up to December 2009, and for the three-months interval January–March 2010, the end of the available time series, as in steps 1–4 above.

[46] Note that the first semester of each year (period of January–June), corresponds approximately to the period when the annual hydrograph at Ladário has its rising limb, while the second semester (period of July–December) corresponds roughly to the recession period.

[47] Figure 8 shows the rmse obtained for each semester and for each model. During the first semester (January–June) when water levels are rising at Ladário, there is not a great deal of difference between rmse values of models 1, 2, and 3 [the second being a simple ARMA$(1, 1)$]. An exception was the year 1993, when model 3 (SARFIMA) clearly showed a better performance than the other two models in this group. But the feature emerging most strongly from the left-hand side of Figure 8 is the much greater range of fluctuations in rmse values associated with model 4, the seasonal SARMA model; in general its performance as measured by rmse was much worse than that of the other three models, although in three years (2001, 2005, and 2009) it performed better than any of the others. The suggested explanation, given above, of the possibility of nonhomogeneity in monthly variances cannot be the whole story, since rmse values of the SARFIMA model, which is also seasonal, do not show the same degree of fluctuation (although inclusion of the long-range dependence parameter D in this fractionally differenced model may have "damped out" fluctuations in forecasts).

[48] A similar picture emerges from the right-hand side of Figure 8, showing rmse values calculated from forecasts, issued in June, for the second semester (July–December) when Ladário water levels are in recession. Except for the two initial years, 1991–1992, the SARMA model shows a much poorer performance, in general, than models 1, 2, and 3, which do not greatly differ in terms of their rmse values. Comparison of the left- and right-hand plots in Figure 8 show that rmse values during recession periods July–December tend to be lower than those found for the rising limb of the water-level hydrograph; we enlarge upon this in the following paragraphs.

[49] In a final analysis, rmse were calculated by comparing observed mean monthly water levels with those predicted by each of the four models. Thus, the 20 forecasts of mean water level in January, February, ..., June (all of which were issued in the preceding December) were compared with the observed mean water levels in those months,

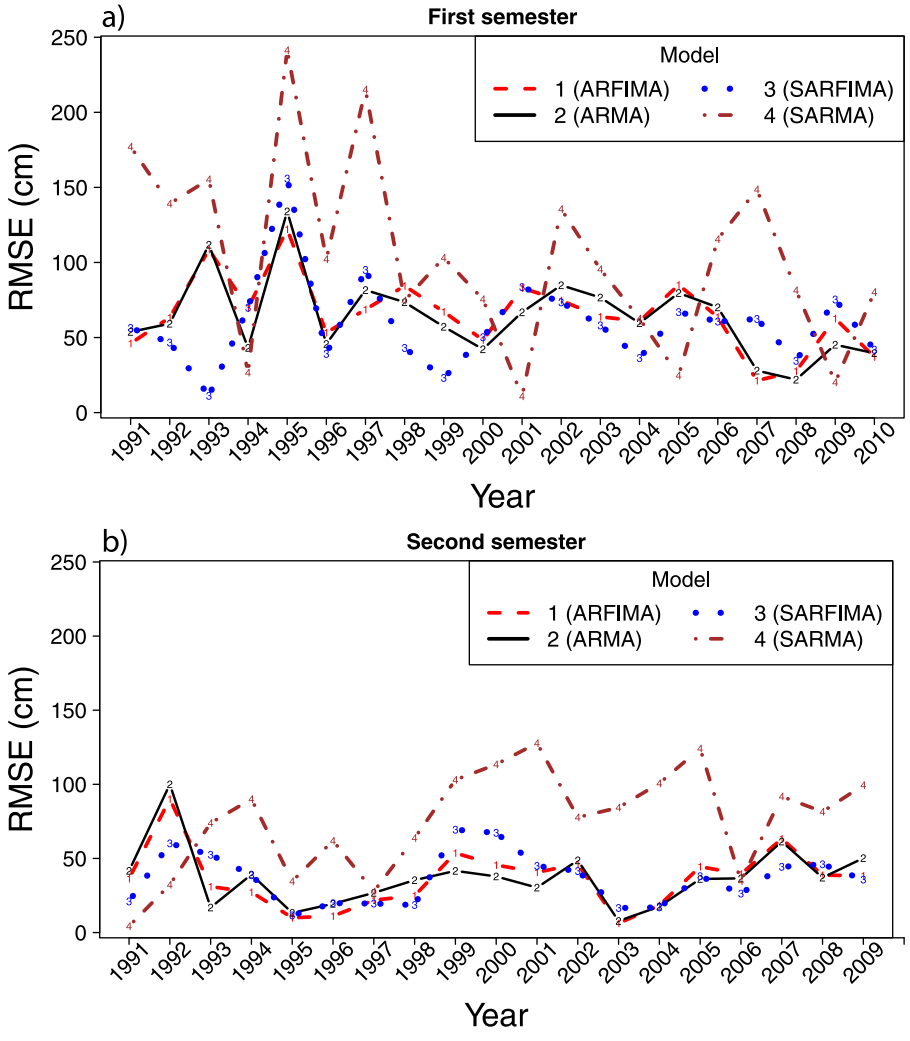

Figure 8. Root mean square error values between the observed and the predicted values, for each year and semester. For each year, the forecasts for the period January–June were issued in December (previous year) and the forecasts for the period July–December were issued in June (current year).

so that the rmse for each month was calculated as the mean of 20 squared differences. A similar procedure was used to calculate rmse for July, August, . . . , December, by comparing the 19 forecasts (issued in the preceding June) with observed water levels in those months.

[50] Figure 9 shows a plot of the rmse calculated from the above procedure, and a number of points stand out clearly from it. First, as suggested Figure 8, the rmse in the second semester July–December, are commonly smaller than those in the first, January–June, the difference being especially marked for model 4 (SARMA). This confirms the point made above, that forecasts appear to be more accurate during the recession, when water levels are falling. Second, for forecasting just one month ahead (January or July, in the two semesters) all four models perform about equally well: but again, the rmse values for July (12.08, 13.58, 11.78, and 15.41 for ARFIMA, ARMA, SARFIMA and SARMA models, respectively) are about half those for January (24.51, 24.45, 23.99, 25.51), for all four models. Third, there is very small difference among models 1, 2, and 3 in either semester, although model 3 is marginally better than the other three models in the three months February–April of the first semester January–June.

7. Final Remarks and Conclusions

[51] The paper has reported results from an analysis of the 110-year time series of mean monthly water levels recorded at Ladário on the Upper Paraguay River, Brazil. A priori considerations suggested that long-range dependence models might be appropriate for forecasting purposes, and two approaches were explored. In the first, the marked seasonal cycle was removed by simple transformation (subtraction of monthly mean, division by monthly standard deviation), with a fractionally differenced model ARFIMA(p,d,q) fitted to the resulting deseasonalized time series. In the second, a seasonal fractionally differenced model with structure SARFIMA$(p,d,q)\times(P,D,Q)_{12}$ was fitted directly to the mean monthly water levels. Having explored all models with p, q, P, Q less than or equal to two, goodness-of-fit criteria suggested the values $p=q=1$ for the ARFIMA model, and $p=2$, $d=0$, $q=0$, $P=0$, $Q=1$ for

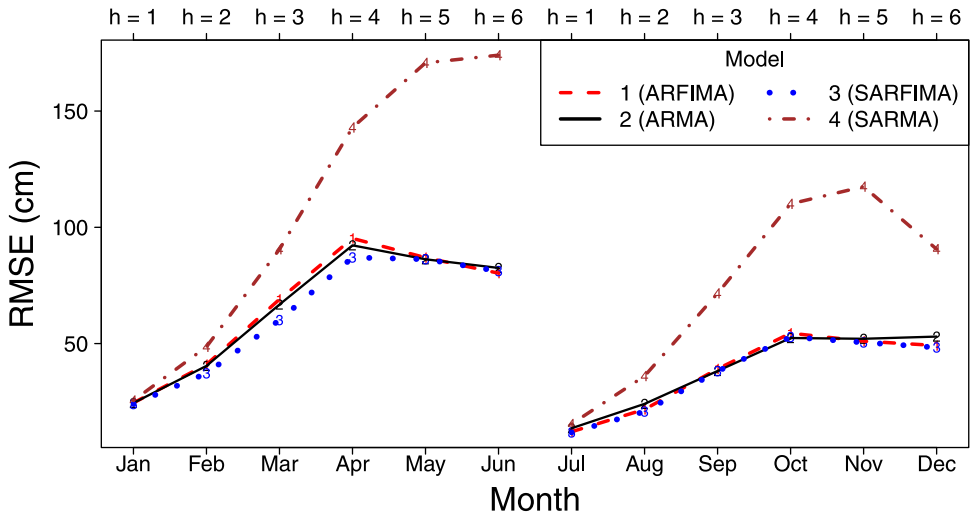

Figure 9. Root mean square error values between the observed and the predicted values for each month. The forecasts for January–June were issued in December (previous year) and the forecasts for July–December were issued in June (current year).

the SARFIMA model. The long-range dependence parameters for the two models were estimated as $d = 0.35 \pm 0.096$ for the ARFIMA model, and $D = 0.439 \pm 0.035$ for the SARFIMA, so that both models showed significant evidence of long-range dependence. When forecasting Ladário water levels up to six months ahead, forecasts given by these two fractionally differenced models were also compared with forecasts given by simpler, "short-range dependence" ARMA(p, q) and SARMA$(p, q) \times (P, Q)_{12}$ models. Performance of the two fractionally-differenced models were compared with the performance of their counterparts in which d and D were set to zero, and which therefore did not model persistence in the series. Beginning in December 1990, each of the four models was used to forecast water levels in the following six-month period January–June; in June 1991, estimates of the parameters in all four models were updated, and forecasts were then "issued" for the period July–December 1991. Thereafter, the procedure of updating estimates of model parameters and the use of the updated models to obtain forecasts up to six months ahead was repeated up to the end of the record some 20 years later. The original values of p, q, P and Q were retained (so that the models were not "reidentified" for each six-month forecasting period). Agreement of forecasts with observation was measured by calculating root mean square errors (rmse); in general, rmse values given by the SARMA model were considerably larger than those given by the other three models [ARFIMA$(1, d, 1)$, ARMA$(1, 1)$ and SARFIMA$(2, 0, 0) \times (0, D, 1)_{12}$], but in general there was little to choose between these three in terms of model performance. The first semester of forecasts, January–June, corresponded to the period of rising water levels at Ladário; the second, July–December, to the period of recession. The performance of all models was better during the recession period than during the period of rising water levels, corresponding to the common observation that forecasting on a hydrographs rising limb is more difficult than on the "smoother" recession.

[52] A limitation of the work is that none of the models includes any causative or explanatory variable. Precipitation would be the obvious explanatory variable to use, but there are no rainfall records (or indeed records of any other type) of a length sufficient to allow fractionally differenced models with explanatory variables to be fitted. A long record of mean monthly discharge (as distinct from the mean monthly water levels at Ladário) is available from 1901 to the present, for the River Paraná at Corrientes, downstream from Ladário and sited after the Paraguay River has joined the Paraná. There is some correlation between the Corrientes flows and the Ladário water levels, so that the latter may show some promise as a predictor of the former. In this case, an ARFIMA model fitted to the deseasonalized time series could be considered as a first choice. However, although the homogeneity of the variances may not be an appropriate assumption, the SARFIMA model is more parsimonious in terms of parameters since it avoids the estimation of 12 monthly means and 12 standard deviations, which are required for deseasonalization. A complication arises because the flows at Corrientes are reconstructed natural flows, adjusted to take account of upstream impoundments and reservoir losses. Alternatively, given the encouraging performance at Ladário of the simple ARMA$(1, 1)$ model (which, as is well-known, exhibits long-range dependence-type behavior when its autoregressive parameters lie close to the unit circle) this model could be considered and the relatively short records available for explanatory variables could then be used for forecasting several months in advance by means of a transfer-function model, not only for the Paraná River at Corrientes, but more widely throughout the la Plata basin.

[53] **Acknowledgments.** T. S. Prass was supported by CNPq-Brazil. S. R. C. Lopes was partially supported by CNPq-Brazil, by CAPES-Brazil, by INCT em *Matemática* and by Pronex *Probabilidade e Processos Estocásticos* – E-26/170.008/2008 – APQ1. The authors are very grateful for constructive remarks by Professor Demetris Koutsoyiannis and two anonymous referees.

References

Arteche, J., and P. M. Robinson (2000), Semiparametric inference in seasonal and cyclical long memory processes, *J. Time Series Anal.*, *21*(1), 1–25.

Assine, M. L. (2005), River avulsions on the Taquari megafan, Pantanal wetland, Brazil, *Geomorphology*, *70*(3–4), 357–371. doi:10.1016/j.geomorph.2005.02.013.

Assine, M. L., and P. C. Soares (2004), Quaternary of the Pantanal, west-central Brazil, *Quat. Int.*, *114*, 23–34, doi:10.1016/S1040-6182(03)00039-9.

Beran, J. (1994), *Statistics for Long Memory Processes*, Chapman and Hall, New York.

Bisognin, C. (2007), Estimação e Previsão em Processos SARFIMA(p, d, q) × (P, D, Q)$_s$ na Presença de Outliers, Ph.D. dissertation, Federal Univ. of Rio Grande do Sul, Porto Alegre, Brazil.

Bisognin, C., and S. R. C. Lopes (2007), Estimating and forecasting the long-memory parameter in the presence of periodicity, *J. Forecasting*, *26*, 405–427.

Bisognin, C., and S. R. C. Lopes (2009), Properties of seasonal long memory processes, *Math. Comput. Model.*, *49*, 1837–1851.

Bordas, M. P. (1996), The Pantanal: An ecosystem in need of protection, *Int. J. Sediment Res.*, *11*(3), 34–39.

Brasil (1997), Plano de Conservação da Bacia do Alto Paraguai (Pantanal) PBAP: Análise integrada e prognóstico da Bacia do Alto Paraguai, *Ministério do Meio Ambiente, dos Recursos Hídricos e da Amazônia Legal*, 369 pp., Brasília, Brazil.

Bravo, J. M., B. Collischonn, D. Allasia, W. Collischonn, A. Villanueva, and C. E. M. Tucci (2005), *Estimating lateral gains and losses in Pantanal rivers* (in Portuguese). I Simpósio de Recursos Hídricos do Sul (AguaSul), ABRH, Santa Maria (RS), Brazil.

Bravo, J. M., D. Allasia, A. R. Paz, W. Collischonn, and C. E. M. Tucci (2012), Coupled hydrologic-hydraulic modeling of the Upper Paraguay River basin, *J. Hydrolog. Eng.*, *17*(5), doi:10.1061/(ASCE)HE.1943-5584.0000494, in press.

Brockwell, P. J., and R. A. Davis (1991), *Time Series: Theory and Method*, 2nd ed., Springer, New York.

Crato, N., R. R. Linhares, and S. R. C. Lopes (2010), Statistical properties of detrended fluctuation analysis, *J. Stat. Comput. Simul.*, *80*, 625–641.

Crato, N., R. R. Linhares, and S. R. C. Lopes (2011), α-stable laws for non-coding regions in DNA sequences, *J. Appl. Stat.*, *38*(2), 261–271.

Darwin C. (1839), *Journal and Remarks, 1832–1835*: Vol. 3 of *Narrative of the Surveying Voyages of His Majesty's Ships Adventure and Beagle* (subsequently published as *The Voyage of the Beagle*), [Available at: http://www.infidels.org/library/historical/charles_darwin/voyage_of_beagle/Chapter7.html], H. Colburn, London.

Elek, P., and L. Márkus (2004), A long range dependent model with nonlinear innovations for simulating daily river flows, *Nat. Hazards Earth Syst. Sci.*, *4*, 277–283.

Giraitis, L., and R. Leipus (1995), A generalized fractionally differencing approach in long-memory modeling, *Lithuanian Math. J.*, *35*(1), 53–65.

Granger, C. W. J. (1980), Long memory relationships and the aggregation of dynamic models, *J. Econom.*, *14*, 227–238.

Granger, C. W. J., and R. Joyeux (1980), An introduction to long memory time series models and fractional differencing, *J. Time Ser. Anal.*, *1*(1), 15–29.

Grimaldi S. (2004), Linear parametric models applied on daily hydrological series, *J. Hydrolog. Eng.*, *9*(5), 383–391.

Hamilton, S. K. (2002), Human impacts on hydrology in the Pantanal wetland of South America, *Water Sci. Technol.*, *45*(11), 35–44.

Hamilton, S. K., S. J. Sippel, and J. M. Melack (1996), Inundation patterns in the Pantanal wetland of South America determined from passive microwave remote sensing, *Arch. Hydrobiol.*, *137*(1), 1–23.

Hassler, U. (1994), (Mis)specification of long memory in seasonal time series, *J. Time Ser. Anal.*, *15*(1), 19–30.

Hipel, K. W., and A. I. McLeod (1994), *Time Series Modelling of Water Resources and Environmental Systems*, Elsevier, New York.

Hirpa, F. A., M. Gabremichael, and T. M. Over (2010), River flow fluctuation analysis: Effect of watershed area, *Water Resour. Res.*, *46*, W12529, doi:10.1029/2009WR009000.

Hosking, J. R. M. (1981), Fractional differencing, *Biometrika*, *68*(1), 165–176.

Hosking, J. R. M. (1984), Modelling persistence in hydrological time series using fractional differencing, *Water Resour. Res.*, *20*(12), 1898–1908.

Hurst, H. E. (1951), Long-term storage in reservoirs, *Trans. Am. Soc. Civil Eng.*, *116*, 770–799.

Junk, W. J., C. N. Cunha, K. M. Wantzen, P. Petermann, C. Strüssmann, M. I. Marques, and J. Adis (2006), Biodiversity and its conservation in the Pantanal of Mato Grosso, Brazil, *Aquat. Sci.*, *68*, 278–309, doi:10.1007/s00027-006-0851-4.

Livina, V., Y. Ashkenazy, Z. Kizner, and S. Havlin (2003), A stochastic model of river discharge fluctuations, *Physica A*, *330*(1–2), 283–290.

Montanari, A., R. Rosso, and M. S. Taqqu (1997), Fractionally differenced ARIMA models applied to hydrologic time series: Identification, estimation, and simulation, *Water Resour. Res.*, *33*(5), 1035–1044.

Montanari, A., R. Rosso, and M. S. Taqqu (2000), A seasonal fractional ARIMA model applied to the Nile River monthly flows at Aswan, *Water Resour. Res.*, *36*(5), 1249–1259.

Mudelssee, M. (2007), Long memory of rivers from spatial aggregation, *Water Resour. Res.*, *43*(1), W01202, doi:10.1029/2006WR005721.

O'Connell, P. E. (1973), Stochastic modelling of long-term persistence in streamflow sequences, Ph.D. Dissertation, Imperial College, London, U.K.

Palma, W. (2007), *Long-Memory Time Series—Theory and Methods*, John Wiley, Hoboken, NJ.

Paz, A. R., W. Collischonn, C. E. M. Tucci, and C. R. Padovani (2011), Large-scale modelling of channel flow and floodplain inundation dynamics and its application to the Pantanal (Brazil), *Hydrol. Processes*, *25*, 1498–1516.

Peiris, M. S., and N. Singh (1996), Predictors for seasonal and nonseasonal fractionally integrated ARIMA models, *Biometrika*, *38*(6), 741–752.

Peng, C., S. V. Buldyrev, A. L. Goldberger, S. Havlin, F. Sciortino, M. Simons, and H. E. Stanley (1992), Long-range correlations in nucleotide sequences, *Nature*, *356*, 168–170.

Porter-Hudak, S. (1990), An application of the seasonal fractionally differenced model to the monetary aggregates, *J. Am. Stat. Assoc.*, *85*(410), 338–344.

Ray, B. K. (1993), Long-range forecasting of IBM product revenues using a seasonal fractionally differenced ARMA model, *Int. J. Forecasting*, *9*, 255–269.

Reisen, V. A., and S. R. C. Lopes (1999), Some simulations and applications of forecasting long-memory time series models, *J. Stat. Plan. Inference*, *80*(2), 269–287.

Reisen, V. A., M. R. Sena Jr., and S. R. C. Lopes (2001), Error and model misspecification in ARFIMA process, *Braz. Rev. Econ.*, *21*(1), 101–135.

Sena, M. R., Jr., V. A. Reisen, and S. R. C. Lopes (2006), Correlated errors in the parameters estimation of ARFIMA model: A simulated study, *Commun. Stat. Simul. Comput.*, *35*(2), 789–802.

Tucci, C. E. M., F. Genz, and R. T. Clarke (1999), Hydrology of the Upper Paraguay Basin, in *Management of Latin American River Basins: Amazon, Plata and São Francisco*, edited by K. Biswas, et al., pp. 103–122, United Nations University Press, Tokyo.

Tucci, C. E. M., A. Villanueva, W. Collischonn, D. G. Allasia, J. M. Bravo, and B. Collischonn (2005), *Projeto Implementação de Práticas de Gerenciamento Integrado de Bacia Hidrográfica para o Pantanal e Bacia do Alto Paraguai, Subprojeto 5.4 - Modelo Integrado de Gerenciamento Hidrológico da Bacia do Alto Paraguai*, ANA/GEF/PNUMA/OEA, Porto Alegre, Brazil.

Tyralis, H., and D. Koutsoyiannis (2011), Simultaneous estimation of the parameters of the Hurst-Kolmogorov stochastic process, *Stochastic Environ. Res. Risk Assess.*, *25*(1), 21–33.

Whittle, P. (1953), *Hypothesis Testing in Time Series Analysis*, Hafner, New York.

J. M. Bravo, R. T. Clarke, and W. Collischonn, Instituto de Pesquisas Hidráulicas, Universidade Federal do Rio Grande do Sul (UFRGS), Porto Alegre-RS, Brazil. (jumarbra@iph.ufrgs.br; clarke@iph.ufrgs.br; collischonn@iph.ufrgs.br)

S. R. C. Lopes and T. S. Prass, Instituto de Matemática, Universidade Federal do Rio Grande do Sul (UFRGS), Porto Alegre-RS, Brazil. (silvia.lopes@ufrgs.br; taianeprass@gmail.com)